16th World Conference on Earthquake, 16WCEE 2017
Santiago Chile, January 9th to 13th 2017
Paper N° 2530 (Abstract ID)
Registration Code: S-Q1464710736

ANALYTICAL MODEL FOR SLAB-COLUMN CONNECTIONS SUBJECTED TO CYCLICALLY INCREASING DRIFTS

I.-S. Drakatos[(1)], K. Beyer[(2)], A. Muttoni[(3)]

[(1)] PhD Candidate, École Polytechnique Fédérale de Lausanne, IBETON, ioannis-sokratis.drakatos@epfl.ch
[(2)] Assistant Professor, École Polytechnique Fédérale de Lausanne, EESD, katrin.beyer@epfl.ch
[(3)] Professor, École Polytechnique Fédérale de Lausanne, IBETON, aurelio.muttoni@epfl.ch

Abstract

Reinforced concrete (RC) flat slabs supported on columns are one of the most widely used structural systems for office and industrial buildings. In regions of medium to high seismic risk RC walls are typically added as lateral force resisting system and to increase the lateral stiffness and strength. Although slab-column connections possess low stiffness and do not contribute substantially to the lateral resistance of the structure, each connection must have the capacity to follow the seismically induced lateral displacements of the building while maintaining the capacity to transfer the vertical loads from the slab to the columns. Otherwise brittle punching failure of the slab occurs and the deformation capacity of the connection determines the deformation capacity of the entire building.

This article presents an analytical model to account for the hysteretic behaviour and cumulative damage effects on the moment-rotation relationship of internal slab-column connections without transverse reinforcement when subjected to cyclic loading. The developed model is an extension of a mechanical model proposed earlier by the authors for monotonic loading conditions. The cyclic model assumes that a fixed shear crack governs the behaviour of the slab-column connection and adopts a hysteretic moment-curvature relationship for the radial direction. The main assumptions of the model are based on local deformation measurements from tests. Seismic damage is introduced through a non-cumulative model proposed by others.

The model performance is assessed through comparison to tests performed by the authors. The cyclic model predictions are in good agreement with the experimental results and provide higher accuracy than the monotonic model with respect to both the local behaviour and the global behaviour.

Keywords: slab-column connections; punching failure; seismic damage; cyclic loading

1 Introduction

In many countries around the world, RC flat slabs supported on columns are one of the most widely used structural systems for office and industrial buildings. This system has the advantage to result in large open floor spaces as well as short construction times and therefore low construction costs. To increase the horizontal stiffness and strength of the structural system, RC walls such as core walls around lift shafts and staircases are typically added to the structural system. The largest portion of the horizontal loads generated during earthquakes will be carried by the walls rather than the columns. However, each slab-column connection must have the capacity to follow the lateral displacements imposed on the building by the earthquake loading while maintaining the capacity to transfer the vertical loads from the slab to the columns. Otherwise, brittle punching failure of the slab occurs and the deformation capacity of the entire building is limited by the deformation capacity of the slab-column connection if the building is not designed to resist progressive collapse.

The seismic design and assessment of structures with flat slabs and columns requires as input estimates of the moment-rotation relationship and the rotation capacity of slab-column connections. Until today, research efforts on slab-column connections with unbalanced moment concentrated on the derivation of empirical relationships between the normalised shear force acting on the slab and the rotation capacity of the slab-column connection [1, 2].

An analytical model has been developed for calculating the moment-rotation relationship under monotonic loading conditions [3, 4]. Experiments on slabs subjected to constant vertical load and monotonically or cyclically increasing moment [5] have shown that cyclic loading can lead to significant degradation and consequently reduction of the moment strength and the corresponding connection rotation determined through monotonic tests (Fig. 1). The monotonic model tends to overestimate the moment strength and the deformation capacity of slab-column connections subjected to cyclically increasing drifts.

This paper presents a model for considering the degradation due to cyclic loading when calculating the moment-rotation relationship of internal slab-column connections without transverse reinforcement. The developed model is an extension of the monotonic mechanical model [3, 4] and its assumptions are based on local deformation measurements from experiments [5].

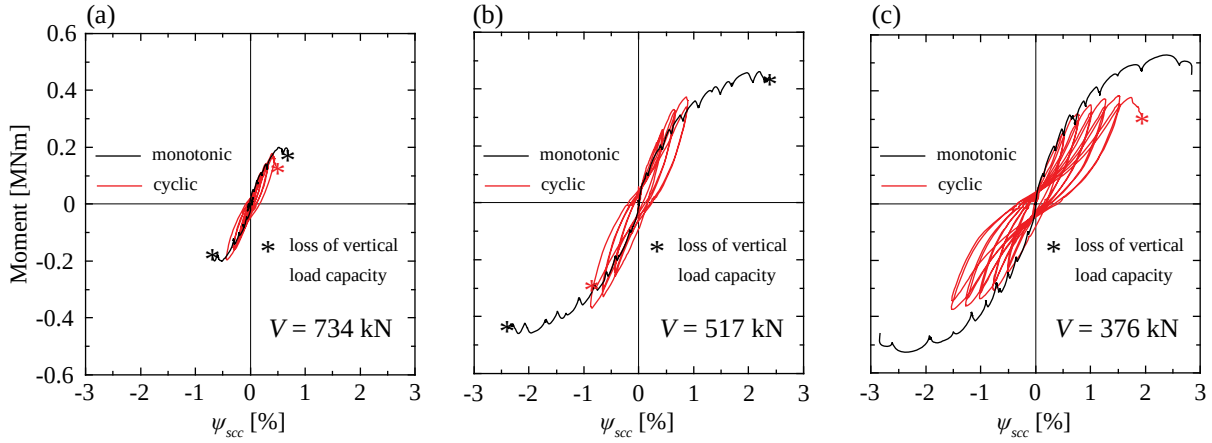

Fig. 1 – Moment-connection rotation for cyclic and monotonic for ρ = 0.75% and different vertical loads [5].

2 Local deformation measurements from tests

This section presents several local deformation measurements based on tests carried out by the authors [5]. The main objective is to identify trends and correlations that are valuable for developing hysteretic models for slab-column connections subjected to combined vertical load and unbalanced moment. This information will be used later in the paper to extend the monotonic analytical model [3, 4] to account for the effect of loading history.

2.1 Correlation between shear crack inclination and top reinforcement yielding

Fig. 2 shows the shear crack inclination for monotonic and cyclic tests performed by the authors [5]. Fig. 3 shows the measured strain at specified locations of the top reinforcement, as function of the unbalanced moment.

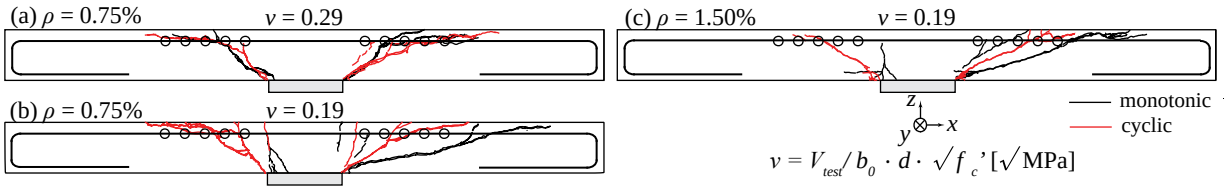

Fig. 2 – Saw cuts for slabs tested under monotonically and cyclically increasing moments and locations where reinforcement strains were measured

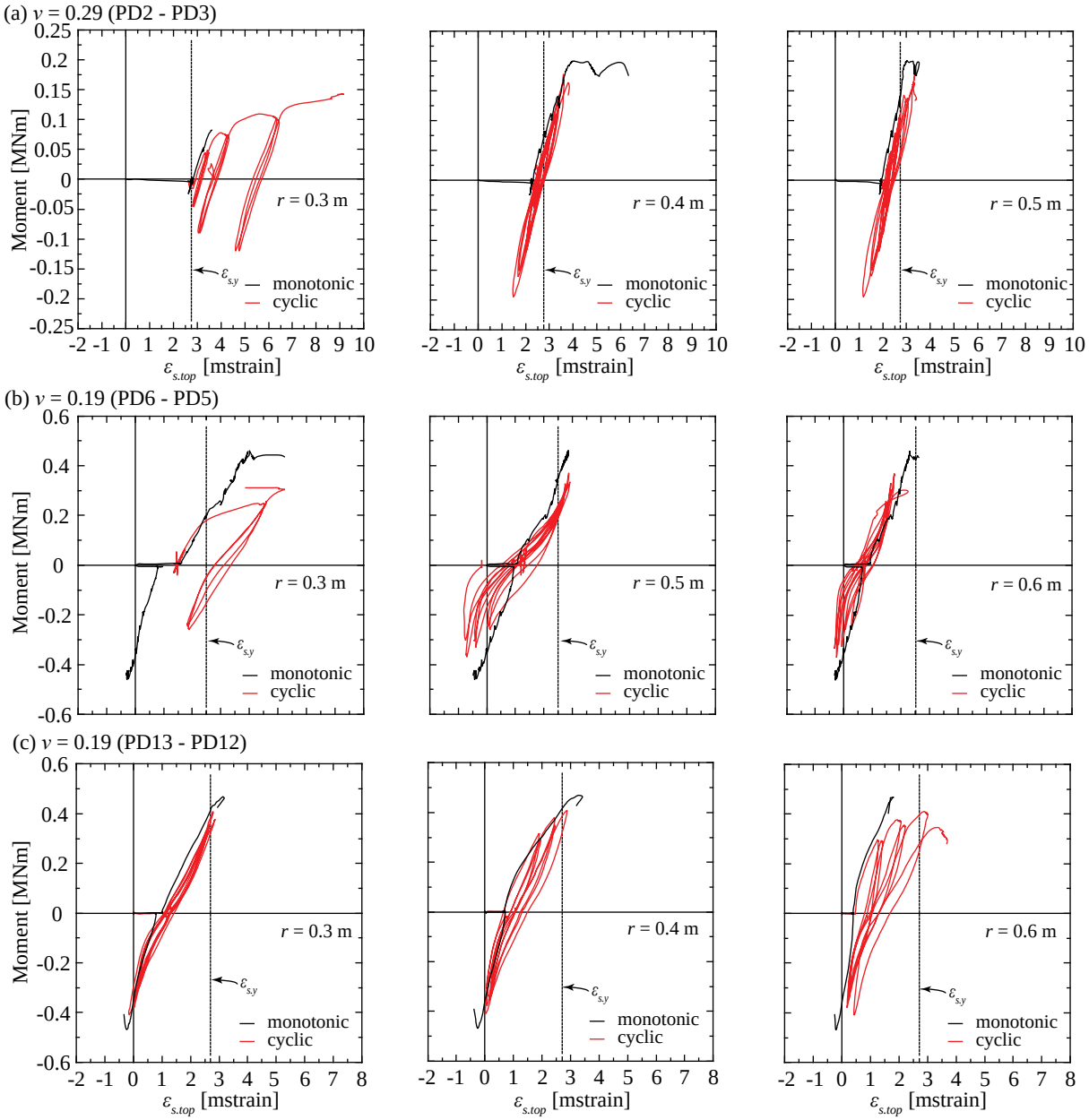

Fig. 3 – Strain gauge measurements at specified locations of top reinforcing bars along the *x*-axis for monotonic and cyclic tests: (a) ρ = 0.75% - v = 0.29, (b) ρ = 0.75% - v = 0.19, (c) ρ = 1.50% - v = 0.19 [5].

For slab PD2 which responded in the inelastic range already under vertical load, Fig. 3a shows that the shear crack was already open after the vertical load application and, therefore, no steeper shear crack could appear during the unbalanced moment introduction. Fig. 2a shows that for both monotonic and cyclic tests the radius at which the shear crack crosses the top reinforcement is $r_0 \approx r_c + d$, where r_c is the column radius and d is the slab effective depth. Shear cracks steeper than 45 degrees were not observed from the saw cuts prepared after the tests have been completed.

For slabs that responded in the elastic range under vertical load but in the post-elastic range during the unbalanced moment introduction, a correlation trend was identified between shear crack inclination and eccentricity at first post-elastic peak. For slab PD6 (ρ = 0.75% - v = 0.19), Fig. 3b shows that vertical load induced only elastic strains while first unloading from post-elastic reinforcement strains occurred at eccentricity $e = M/V$ = 0.62 m, which is rather close to the experimentally observed shear crack inclination at failure from Fig. 2b (r_0 = 0.56 m). For slab PD13 (ρ = 1.50% - v = 0.19), first unloading from post-elastic reinforcement strains occurred at e = 0.75 m (Fig. 3c). This eccentricity is close to the experimentally observed radius where the shear crack crosses the reinforcement, which can be taken from Fig. 2c (r_0 = 0.68 m).

Based on these observations, one can conclude that the cyclic behaviour of slab-column connections responding into the inelastic range is dominated by the opening-closing of a fixed shear crack rather than a rotating shear crack, which was observed for monotonic tests and adopted by the analytical model for monotonically increasing drifts [3]. The radius at which this single shear crack crosses the top flexural reinforcement correlates rather well with the eccentricity of the slab-column connection at first unloading from the post-elastic range. The lower-bound radius at which the top reinforcement is crossed by the shear crack is $r_c + d$ (i.e. distance d from the column edge, Fig. 2).

2.2 Shear crack opening-closing process

The shear crack opening-closing process was monitored using slab thickness variation measurements. Fig. 4a, b show the influence of the loading history on the measured crack openings in the connection proximity (r = 0.25 m) for different gravity loads and reinforcement ratios. For comparison purposes the shear force-stirrup strain of a cantilever T-beam tested by Ma et al. under cyclic shear [6] is shown in Fig. 4c.

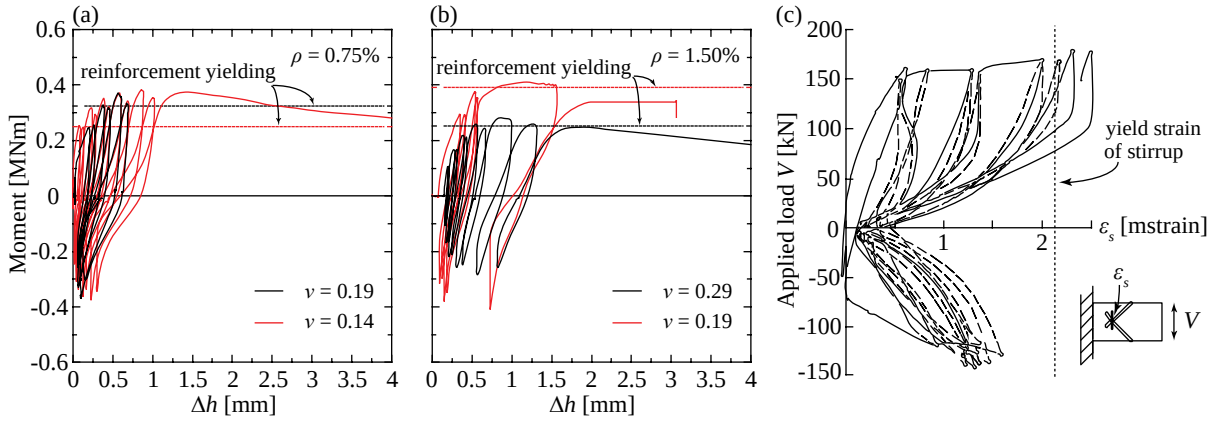

Fig. 4 – Comparison of measured thickness variation between cyclically tested slabs for different gravity loads along the strong axis (r = 0.25 m): (a) ρ = 0.75% and (b) ρ = 1.50%. (c) Shear force - stirrup strain for a T-beam subjected to cyclic shear [6].

For T-beams subjected to cyclic shear, the recorded stirrup strain attains values close to zero for small applied loads while the V - ε_s curve has very small stiffness for near zero shear force V (Fig. 4c). Therefore, it can be deduced that the stirrup strain is suppressed and the shear crack closes. Loading in the reverse direction leads to tension in the reinforcement of the opposite side and opening of a shear crack perpendicularly to the previously closed one. On the contrary, Fig. 4a and b show that for the tested slabs [5] the thickness variation at

zero unbalanced moment is larger than zero. This indicates that the shear crack opening is not suppressed during loading in the opposite direction.

The measurement of the crack opening can also provide better insight into the accumulation of plastic crack openings and plastic rotations that are associated with them, which influence significantly the cyclic behaviour of slab-column connections. As can be seen from Fig. 4, during unloading-reloading in the elastic range, crack openings due to moment introduction are recovered, with minor unrecoverable crack openings being attributed to the negative tension stiffening effect. Yield crack opening corresponds to the beginning of reinforcement yielding (Section 2.1). Post-yield behaviour is characterised by appearance of plastic crack openings, which correspond to plastic reinforcement strains. For loading in the post-elastic range, increase of plastic rotations is assumed to occur after reaching the peak rotation of the previous cycle in the same direction. This assumption is consistent with the definition of plastic crack opening for monotonic loading and has already been adopted by others [7]. Table 1 compares the elastic crack opening (or thickness variation) for the cycle before the peak unbalanced moment M_{max} (Δh_{el}) and the crack opening difference between positive and negative peak at M_{max} (Δh_p^+- Δh_p^-) for the specimens for which crack opening measurements were available. Comparison of columns 2 and 5 of Table 1 shows that at M_{max} no compression of plastic crack openings occurred for the tested slab-column connections during unloading and loading in the opposite direction.

Table 1 – Elastic crack opening and difference between peak crack openings at M_{max} for the cyclic tests for which crack opening measurements were available (sorted by increasing vertical load and reinforcement ratio)

Slab Name	Δh_{el} [mm]	Δh_p^+ [mm]	Δh_p^- [mm]	Δh_p^+- Δh_p^- [mm]
PD8	0.57	0.82	0.24	0.58
PD6	0.39	0.57	0.17	0.40
PD13	0.75	1.54	0.74	0.80
PD11	0.30	0.86	0.56	0.30

3 Hysteretic moment-rotation relationship

As observed by Vaz Rodriguez [8], specimens subjected to concentrated loads may significantly increase their crack widths when they are subjected to cyclic loading. The amount of shear force that can be carried by a slab (for the same level of gravity loads) may thus be reduced under earthquake conditions. Up to date, there is no suitable model to assess the increase of crack widths on RC slab-column connections when they are subjected to cyclic unbalanced moments.

In the analytical model for the load-rotation relationship of slabs subjected to vertical loads alone [9], the slab is divided into an even number *n* of sector elements and the region inside the shear crack. A quadri-linear moment-curvature relationship is adopted for both the radial and the tangential moments accounting for the influence of the shear crack on the flexural behaviour in a computationally efficient way. This model forms the basis of the analytical model for the moment-rotation relationship of slabs under monotonically increasing drifts [3]. Extending this model for cyclic loading conditions is considerably facilitated if a hysteretic moment-curvature relationship is adopted. This simplified extension to predict the increase of crack widths in the proximity of slab-column connections when subjected to cyclic loading is presented in this section. The assumptions regarding the shear crack inclination are presented first, followed by the assumptions related to the hysteretic moment-curvature relationship. Finally, the adopted approach for the consideration of the seismic damage is presented. It should be noted that the same formulas used for the calculation of the monotonic moment-rotation curve [3, 4] apply also for the calculation of the cyclic moment-rotation curve and are not repeated in the following.

3.1 Shear crack inclination

If during loading and reloading no yielding occurs, no plastic radial curvatures appear and the shear crack opening due to unbalanced moment is assumed to be recovered completely during the unloading that follows.

Therefore, for this case, the radius of the shear crack (r_0) is assumed to be equal to the attained eccentricity at that load step, like for monotonic loading conditions [3].

Concerning the shear crack inclination of cyclically loaded slab-column connections responding beyond the yield limit, a fixed value for the radius r_0 is assumed, which corresponds to the shear crack inclination at the first post-yield peak. This assumption is based on experimental observations of the slab saw cuts and recorded reinforcement strains presented previously (§ 2.1). For subsequent loading and unloading in both directions, it is assumed that all additional plastic curvatures of the considered sector element are concentrated at this fixed shear crack. Since this crack is assumed to govern the behaviour of each sector element of the slab-column connection during all subsequent cycles, no flatter or steeper shear crack can appear.

3.2 Moment-curvature relationship

This paper proposes to account for the hysteretic behaviour of slab-column connections by adopting a hysteretic moment-curvature relationship only for the radial moments acting on the shear crack ($r = r_0$). Unlike for the case of monotonic loading, for which the radial moment of each sector element depends only on the corresponding radial curvature [3], for cyclic loading it is assumed that the radial moment depends also on the loading history as will be shown in the following. Both the axisymmetric model for slabs subjected to vertical load alone [9] and the analytical model for slabs subjected to combined vertical load and monotonically increasing unbalanced moment [3] adopt a piece-wise linear (quadri-linear) moment-curvature relationship for the sector elements. Likewise, the hysteretic M - χ relationship presented in the following adopts a piece-wise linear form (polygonal shape). Adoption of a smooth hysteretic model would add significant and unjustified complexity to the calculation and would be inconsistent with the above-mentioned analytical models [9, 3]. An additional assumption to describe the increase-decrease of the developed plastic radial curvature to simulate the opening-closing process of the shear crack is necessary and will be presented in the following.

Fig. 5 shows the assumed hysteretic moment-curvature relationship (colored lines) and the primary moment-curvature relationship (black line). The shape of the unloading-reloading branches is based on a hysteretic shear model for concrete members by Ozcebe and Saatcioglu [10]. Positive and negative directions correspond to increasing tension in the top reinforcement and decreasing compression in the bottom reinforcement, respectively (see Fig. 5). To facilitate understanding, the hysteresis loops are shown for four post-elastic scenarios depending on the sign of the radial moment at negative peak ($m_{rad..peak}$-) and the sign and value of the corresponding curvature ($\chi_{rad..peak}$-). It should be noted that the moment-rotation curve represents the global behaviour of the slab-column connection, whereas the shown m_{rad} - χ_{rad} relationship is formulated for each sector element. Therefore the loading and unloading branches of the m_{rad} - χ_{rad} curve do not necessarily correspond to the loading and unloading branches of the moment-rotation curve.

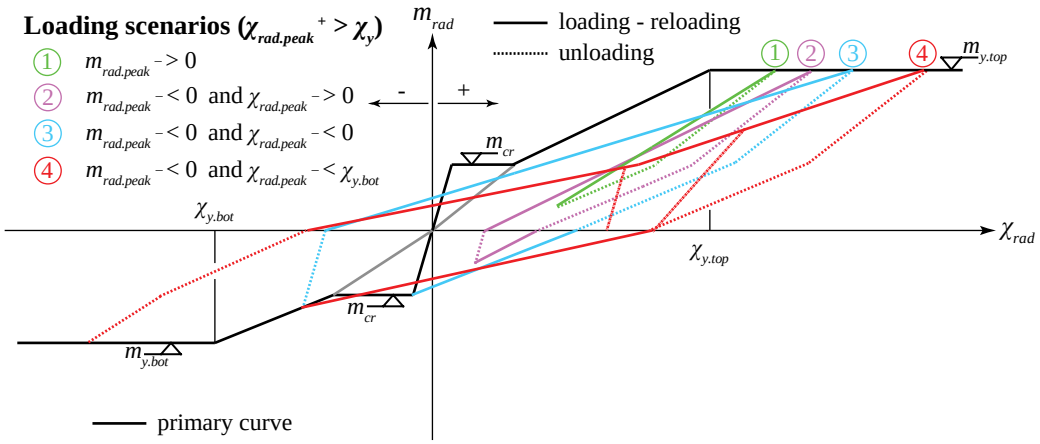

Fig. 5 – Proposed hysteretic radial moment-curvature relationship for each sector element of the slab (based on Ozcebe and Saatcioglu [10]).

3.2.1 Unloading branches

The following rules are applied for the loop segments that correspond to unloading:

1. Unloading follows the primary curve (black line in Fig. 5) if $\chi < \chi_y$ at the beginning of unloading and m_{cr} has not been previously exceeded in either direction.
2. If m_{cr} has been exceeded at least once in the considered direction and the yield curvature has not been previously exceeded in the opposite direction ($\chi < \chi_y$), unloading from $m_{rad.peak} > m_{cr}$ follows the elastic post-cracking stiffness (grey line in Fig. 5) up to the zero radial moment axis. If $m_{rad.peak} < m_{cr}$, unloading follows the initial stiffness up to zero radial moment. If the yield curvature has already been exceeded in the opposite direction, unloading follows the initial stiffness up to zero radial moment independently from the value of $m_{rad.peak}$.
3. If the yield curvature has been exceeded at least once in the considered quadrant, unloading from curvature higher than the maximum previously attained curvature follows the elastic post-cracking stiffness until m_{cr}. Unloading for $m_{rad} < m_{cr}$ follows a line connecting m_{cr} with the plastic radial curvature χ_{pl} of the considered sector element (zero radial moment). If the peak curvature is smaller than the maximum previously attained curvature, unloading follows the initial stiffness up to $m_{rad} = 0$ if $\chi < \chi_{pl}$, otherwise a line connecting $\chi_{rad.peak}$ with χ_{pl} is followed (dash-dotted lines in Fig. 5).
   The plastic radial curvature $\chi_{pl.i}(\varphi_i)$ of the sector element at angle φ_i is calculated according to the following rules:

   - For the first unloading from the post-yield curvature:

$$\chi_{pl.i}(\varphi_i) = \chi_{peak.i}(\varphi_i) - \chi_y(\varphi_i) \quad (1)$$

     where χ_y is the yield curvature of the sector element, calculated according to Muttoni [9].

   - If the yield curvature has been previously exceeded in the considered direction, increase of the plastic radial curvatures due to tensile strains in the top or bottom reinforcement during loading in the positive direction ($m_{rad} > 0$) or in the negative direction ($m_{rad} < 0$), respectively, can occur only for curvatures higher than the previously attained curvatures in that direction:

$$\chi_{pl.i}(\varphi_i) = \left[\chi_{peak.i}(\varphi_i) - \chi_{peak.i-1}(\varphi_i)\right] - \chi_{pl.i-1}(\varphi_i) \quad (2)$$

3.2.2 Loading and reloading branches

With regard to the loop segments that correspond to loading and reloading, the following rules are applied:

1. Loading and reloading in both directions follow the primary curve until unloading from the post-cracking branch occurs.
2. If unloading is terminated prior to reaching the zero moment axis, reloading in the same quadrant follows a straight line aiming at the previously attained moment in the same direction both for moment at negative peak higher or smaller than m_{cr} (green line in Fig. 5). Further loading follows the primary curve.
3. If the considered sector element has not been previously loaded beyond the cracking moment in the considered direction, loading-reloading targets the cracking moment m_{cr}, even if plastic curvatures have been previously developed during loading in the opposite direction (purple and blue line in Fig. 5). Further loading follows the primary curve.
4. If the considered sector element has been previously loaded beyond the cracking moment in the considered direction, reloading aims at the previously attained moment in the same direction (red line in Fig. 5). Further loading follows the primary curve.
5. If the yield curvature has been previously exceeded in the direction with the lowest radial moment (bottom reinforcement under tension), reloading towards the direction with the highest radial moment

(top reinforcement in tension) follows the same stiffness as for reloading in the opposite direction (see Fig. 5) up to suppression of plastic curvatures of the reinforcement previously in tension (bottom reinforcement). The plastic curvature locked in the sector element (at angle φ_i with respect to the bending axis) due to sagging radial moment is reduced according to the following formula:

$$\chi_{pl.bot}(\varphi_i) = \left[\chi(\varphi_i) - \chi_{y.bot}(\varphi_i)\right] - \chi_{pl.bot.peak}(\varphi_i) \leq 0 \quad (3)$$

where $\chi_{y.bot}(\varphi_i)$ is the yield curvature for bottom reinforcement in tension and $\chi_{pl.bot.peak}(\varphi_i)$ is the plastic curvature at the previous peak that is locked in the sector element due to tensile strains in the bottom reinforcement ($\chi_{y.bot}(\varphi_i)$, $\chi_{pl.bot.peak}(\varphi_i) > 0$ in Eq. 3).

Further loading aims at the previously attained peak moment in the same direction (red line in Fig. 5).

3.3 Seismic damage

In order to consider both the stiffness degradation and the strength degradation when calculating the moment-curvature relationship of each sector element, a seismic damage model should be incorporated. This paper adopts the Modified Flexural Damage Ratio (MFDR) as proposed by Roufaiel and Meyer [11] (Fig. 6a).

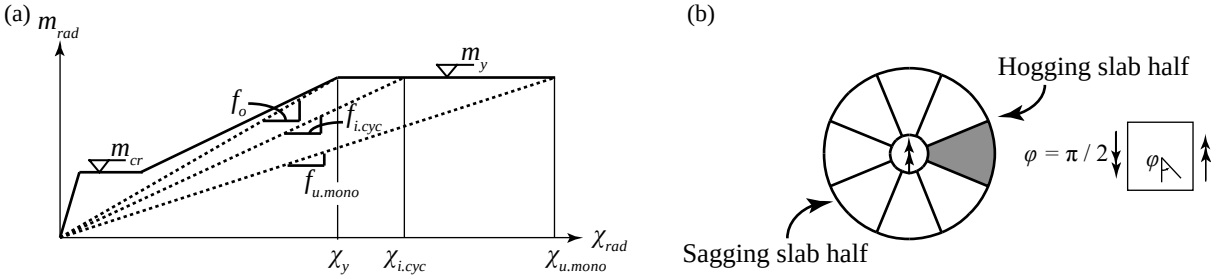

Fig. 6 – Adopted model for seismic damage of slab-column connections (based on Roufaiel and Meyer [11]).

For the calculation of the seismic damage according to [11] only the secant flexibility (inverse of secant stiffness - Fig. 6a) at punching failure under monotonic loading conditions should be known beforehand for the sector element that is subjected to the largest slab rotations (Fig. 6b), i.e. the tip of the hogging slab half ($f_{u.mono}(\pi/2) = \chi_{u.mono}(\pi/2) \ / \ m_{rad.u.mono}(\pi/2)$). $f_{u.mono}(\pi/2)$ can be calculated using the analytical model for monotonically increasing drifts [3]. Afterwards, the damage index $D(\varphi_i)$ can be computed for each sector element as follows

$$D(\varphi_i) = \frac{f_{j.cyc}(\varphi_i) - f_o(\varphi_i)}{f_{u.mono}(\pi/2) - f_o(\varphi_i)} \quad (4)$$

where f_o is the radial yield flexibility and $f_{j.cyc}(\varphi_i)$ is the secant flexibility at the monotonic (or primary) moment-curvature curve corresponding to the curvature at the peak of cycle j for the sector element at angle φ_i from the bending axis. According to [11] the maximum damage index between positive and negative loading should be taken. Since for slab-column connections subjected to constant vertical load and cyclically increasing moment radial moments are already present after the application of vertical loads, high sagging radial moments could appear only for very low gravity loads and high drift levels. In most realistic cases it is the hogging slab half (positive loading) that determines the seismic damage ratio $D(\varphi_i)$.

It should be noted that the hysteretic moment-curvature relationship described in the previous section allows for calculating the dissipated energy. Therefore, in addition to non-cumulative seismic damage approaches (e.g. [11]), the mechanical model can also accommodate cumulative approaches (e.g. [12]) for the seismic damage of slab-column connections and combined cumulative and non-cumulative approaches (e.g. [13]). However, it should be noted that since the calculation is driven by the global (or connection) rotation and the rotations ψ_{max} and ψ_{min} are calculated to satisfy global equilibrium, the radial curvature at peak for each sector element depends not only on its damage ratio D but also on the damage ratio D of all the other sector elements. Therefore, for the

same connection rotation, the cyclic model predicts smaller unbalanced moment with increasing number of cycles, even if a non-cumulative damage model is adopted.

4 Failure criterion

In the following, a failure criterion for drift-induced punching is proposed, which is based on the failure criterion of the CSCT [9]. The adopted failure criterion assumes that shear force redistribution between adjacent sector elements can occur. Shear redistribution from sector elements with higher rotations to sector elements with smaller rotations has been previously found to influence significantly the punching strength and corresponding rotation of slabs loaded and/or reinforced in a non-axisymmetric manner [14].

Based on the work of Sagaseta et al. on non-axisymmetric punching [14], it is assumed that failure of both monotonically and cyclically loaded slabs occurs when the sum of the shear forces acting on the sector elements of the hogging slab half ($0 \le \varphi \le \pi$) is equal to the sum of the shear resistance of these sector elements:

$$V_{R.hog} = \int_0^{\pi} v_R(\varphi) \cdot (r_c' + d(\varphi))\, d\varphi \tag{5}$$

where r_c' is the nominal radius for shear calculation, which for square columns is adjusted to give the same perimeter, and $v_R(\varphi)$ is the shear resistance per unit length in MN/m:

$$v_R(\varphi) = \frac{0.75 \cdot d(\varphi) \cdot \sqrt{f_c'}}{1 + 15 \cdot \frac{\psi(\varphi) \cdot d(\varphi)}{d_g + d_{g.0}}} \quad \text{(SI Units; N, mm)} \tag{6}$$

where f_c is the concrete compressive strength, d_g is the maximum aggregate size and $d_{g.0}$ is the reference aggregate size, which is assumed to be equal to 16 mm. Note that the effective depth d changes with φ to account for the different effective depths for bending around the x- and y-axis. One can either apply a cosinusoidal interpolation for intermediate angles or use an average value for all angles. The former is applied for the calculations presented in this paper.

5 Experimental validation

The presented model, which has been extended from monotonic to cyclic loading, is compared to five full-scale slabs, which were previously tested by the authors under constant vertical load and cyclically increasing unbalanced moment [5]. The comparison is performed with regard to the inclination of the critical shear crack, the local slab rotation and the moment-rotation response.

5.1 Inclination of the critical shear crack

Fig. 7 compares the saw cut of each cyclically tested slab (drawn in black) with the assumed shear crack inclination at first unloading from the post-elastic range (continuous red lines). To facilitate discussion, the assumed shear crack inclination at punching failure according to the monotonic model [3] is also shown in the same figure (dashed red lines).

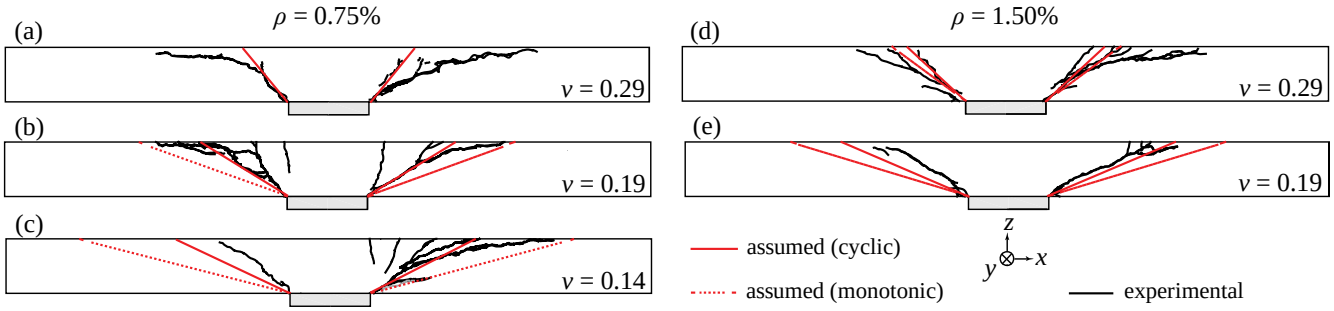

Fig. 7 – Comparison between experimental shear crack inclination (based on saw cuts) and assumed shear crack inclination for the cyclic tests performed by the authors [5].

For low gravity loads (Fig. 7b, c and e), it is shown that by assuming $r_0 = e$ the predicted inclination of the shear crack (dashed red lines) is significantly smaller than the experimentally observed one. On the other hand, the assumption that the eccentricity at the first post-elastic peak determines the inclination of the shear crack during subsequent loading/unloading (continuous red lines) leads to prediction of steeper shear cracks, which agrees better with the experimental results. For high gravity loads (Fig. 7a and d), the assumption that r_0 cannot be smaller than $r_0 + d$ shows good agreement with the results of the cyclic tests. Comparison between the predictions of the monotonic model (dashed black lines) and the cyclic model (continuous black lines) shows that the cyclic model predicts steeper shear crack than the monotonic model. The difference between the predictions of the monotonic model and the cyclic model increases for low gravity loads. These observations are in accordance with the experimental results [5].

5.2 Local slab rotations

Fig. 8 compares the measured and predicted $M - \psi_x$ relationships (x axis as shown in Fig. 7) according to the cyclic analytical model presented previously. It should be noted that maximum values of ψ_x correspond to the maximum slab rotation ψ_{max} whereas minimum ψ_x values correspond to the minimum slab rotation.

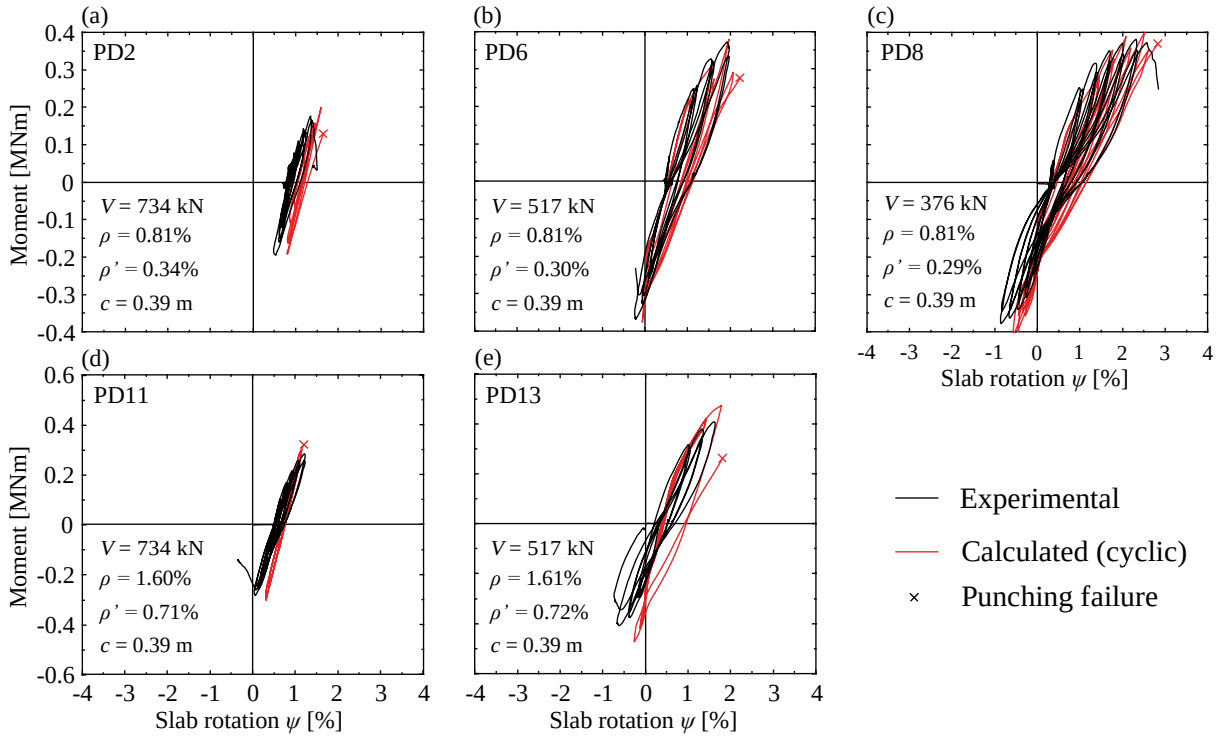

Fig. 8 – Experimental and calculated M - ψ_x curves for the cyclic tests performed by the authors [5].

Fig. 8 shows that the proposed cyclic analytical model gives rather accurate predictions of the maximum and minimum slab rotation of the cyclically tested slabs. In particular, the predictions are more precise for the maximum slab rotations than for the minimum slab rotations. For the minimum slab rotations, the predicted M - ψ curve is stiffer than the experimental one. This can be explained by the fact that according to the model loading towards the negative direction is characterized by stiffer $m_{rad} - \chi_{rad}$ relationship for sector elements that have previously developed smaller plastic rotations than the sector element at the tip of the sagging slab half (ψ_{min}) (Fig. 5 – violet/cyan loops vs red loop).

5.3 Moment strength and deformation capacity

In the following, the experimental moment-rotation response of the cyclically tested slabs [5] is compared to the predicted moment-rotation response according to the proposed cyclic model (Fig. 9). For comparison purposes, the predicted moment-rotation curves according to the monotonic analytical model are also shown in the same figure (dashed curves).

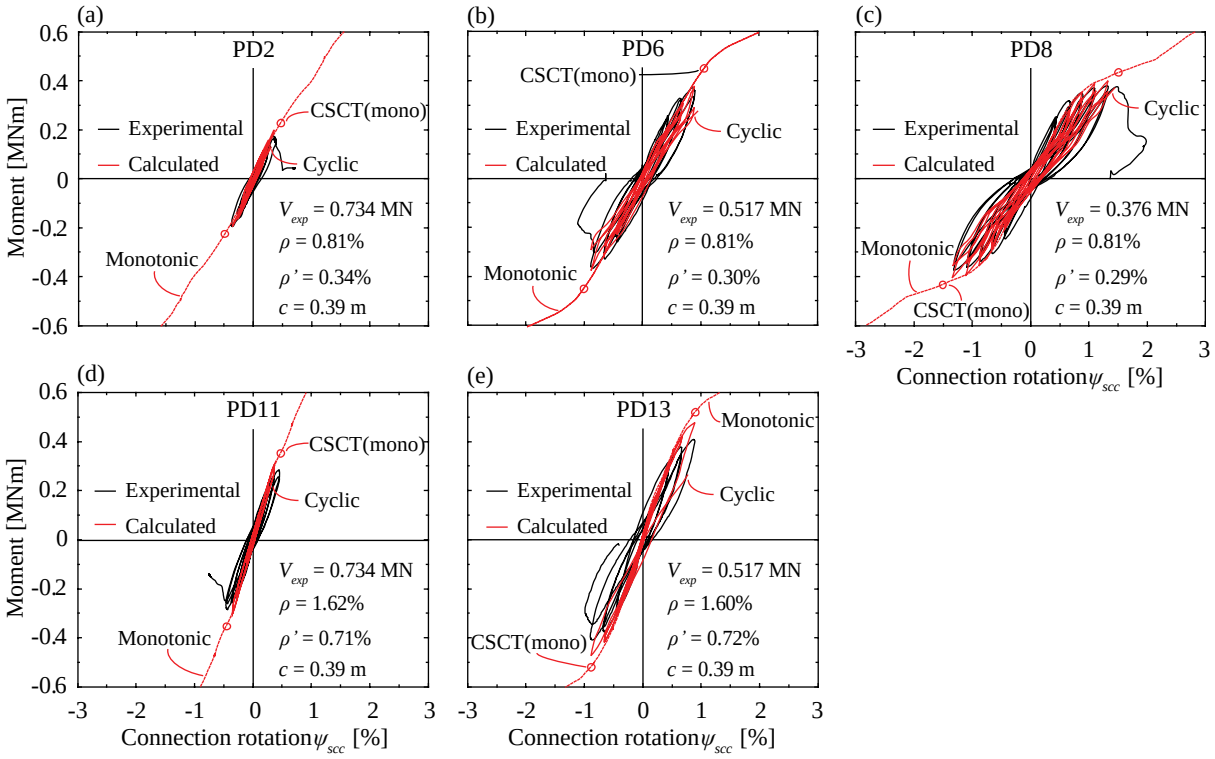

Fig. 9 – Comparison between experimental and calculated moment-connection rotation curves for the cyclic tests performed by the authors [5].

Fig. 9 shows that the cyclic model predicts more accurately the final part of the experimental response than the monotonic model. Moreover, the approach presented in this paper allows for better prediction of both the moment strength and the deformation capacity of the cyclically tested slabs compared to the monotonic model since the effect of loading history is explicitly accounted for.

6 Conclusions and Outlook

This paper presents an analytical model for the calculation of the moment-rotation relationship of slab-column connections under cyclically induced drifts. The model is an extension of a mechanical model proposed earlier by the authors for monotonically increasing drifts. The main additional assumptions of the cyclic model are derived from local-scale experimental observations on slab specimens tested by the authors. The model adopts a hysteretic moment-curvature relationship only for the radial direction while seismic damage is incorporated

through a non-cumulative damage model proposed by others. Comparison with the results of a test campaign conducted by the authors shows that the cyclic model predicts more accurately the local and global response of the tested specimens than the monotonic model.

Comparison of the cyclic model predictions with test results reported in the literature is currently underway. Moreover, implementation of different seismic damage indices is foreseen so as to identify the damage model that best describes the seismic response of slab-column connections. This investigation will reveal whether there is need for a new damage model for slab-column connections.

7 References

[1] Pan A, Moehle JP (1989): Lateral displacement ductility of reinforced concrete flat plates. *ACI Structural Journal*, **86** (3), 250-258.

[2] Hueste MBD, Wight JK (1999): Nonlinear punching shear failure model for interior slab-column connections. *Journal of Structural Engineering ASCE*, **125** (9), 997-1008.

[3] Drakatos IS, Muttoni A, Beyer K (2014): Mechanical model for flexural behaviour of slab-column connections under seismically induced deformations. *Proceedings of the 4th International fib Congress*, Mumbai, India.

[4] Drakatos IS, Beyer K, Muttoni A (2014): Lateral force resisting mechanisms in slab-column connections: An analytical approach. *Proceedings of the 2nd Conference on Earthquake Engineering and Seismology*, Istanbul, Turkey.

[5] Drakatos IS, Muttoni A, Beyer K (2016): Internal slab-column connections under monotonic and cyclic imposed rotations. *Engineering Structures*. (accepted for publication)

[6] Ma SYM, Bertero VV, Popov EP (1976): Experimental and analytical studies on the hysteretic behavior of reinforced concrete rectangular and T-beams. *Report EERC 76-2*, Earthquake Engineering Research Center, Berkeley, USA.

[7] Takeda T, Sozen MA, Nielsen NN (1970): Reinforced concrete response to simulated earthquakes. *Journal of The Structural Division ASCE*, **96**, 2557-2573.

[8] Vaz Rodriguez R (2007): Shear strength of reinforced concrete bridge deck slabs. *PhD Thesis*, EPFL, Lausanne, Switzerland.

[9] Muttoni A. (2008): Punching shear strength of reinforced concrete slabs without transverse reinforcement. *ACI Structural Journal*, **105** (4), 440-450.

[10] Ozcebe G, Saatcioglu M (1989): Hysteretic shear model for reinforced concrete members. *Journal of Structural Engineering ASCE*, **115** (1), 132-148.

[11] Roufaiel MSL, Meyer C (1987): Analytical modelling of hysteretic behaviour of R/C frames. *Journal of Structural Engineering ASCE*, **113** (3), 429-444.

[12] Gosain NK, Brown RH, Jirsa JO (1985): Shear requirements for load reversals on RC members. *Journal of Structural Engineering ASCE*, **103** (7), 1461-1476.

[13] Park YJ, Ang AHS (1985): Mechanistic seismic damage model for reinforced concrete. *Journal of Structural Engineering ASCE*, **111** (4), 722-739.

[14] Sagaseta J, Muttoni A, Fernández Ruiz M, Tassinari L (2011): Non-axis-symmetrical punching shear around internal columns of RC slabs without transverse reinforcement. *Magazine of Concrete Research*, **63** (6), 441-457.